Proc. 3rd Int. Conf. Physics of Solid State Ionics (ICPSSI-3)
J. Phys. Soc. Jpn. **79** (2010) Suppl. A, pp. 163-168

Characterization of PVA-NH_4NO_3 Polymer Electrolyte and its Application in Rechargeable Proton Battery

Subramaniyan SELVASEKARAPANDIAN*, Muthusamy HEMA[1,2], Junichi KAWAMURA[3], Osamu KAMISHIMA[3] and Rangaswami BASKARAN[3]

*Kalasalingam University, Krishnankoil-626 190, Viruthunagar, Tamil nadu, India

[1]Physics Division, BU-DRDO Centre for Life Sciences, Bharathiar University, Coimbatore-641 046, Tamil nadu, India

[2]Solid State and Radiation Physics Laboratory, Department of Physics, Bharathiar University, Coimbatore – 641 046, India.

[3]IMRAM, Tohoku University, Katahira 2-1-1, Aoba-ku, Sendai 980-8577, Japan

(Received September 29, 2009; accepted December 26, 2009)

The PVA-NH_4NO_3 polymer electrolytes have been prepared by solvent casting technique and characterized by XRD, FTIR, DSC, Raman, ^{1}H NMR and ac impedance spectroscopic studies to find out best composition possessing good electrical and mechanical stability. Using the best optimum composition, proton battery with two different cell configurations have been constructed and subjected to rechargeability studies. In the present study rechargeability up to 3 cycles without significant loss in the voltage has been obtained for the cell with configuration Zn + $ZnSO_4.7H_2O$|80PVA: $20NH_4NO_3$ | V_2O_5+PbO_2+ C + PE.

KEYWORDS: polymer electrolyte, solvent casting technique, proton battery

1. Introduction

Within the realm of solid polymer electrolyte, proton conducting polymer electrolytes have become materials of growing interest because of their wide ranging applications in electrochemical devices. Inorganic acids doped systems have been shown to suffer from chemical degradation and mechanical integrity and hence ammonium salt doped system is preferred most for practical applications.

The present work aims at developing a new type of proton conducting polymer electrolyte with 88% hydrolyzed poly (vinyl alcohol), PVA (possessing higher conductivity than 99% hydrolyzed) [1] as the host polymer and ammonium nitrate (NH_4NO_3) as the dopant. Different techniques like XRD, FTIR, DSC, Raman, ^{1}H NMR and ac impedance spectroscopic studies have been used to characterize the prepared polymer electrolytes for its applicability in rechargeable proton battery.

2. Experimental

Preparation of electrolyte: Different compositions of PVA: NH_4NO_3 have been prepared by solvent casting technique using DMSO solvent. The prepared polymer electrolytes are mechanically strong, transparent and flexible with thickness ranging from 0.2 to 0.4μm. X-Ray Diffraction (XRD) patterns were recorded at room temperature on a Philips X'Pert PRO diffractometer. Differential Scanning Calorimetry (DSC) thermograms were obtained using Perkin-Elmer system DSC7 at a heating rate of 5K/min under nitrogen atmosphere. Fourier JASCO spectrophotometer is used in the frequency range 600 cm^{-1} to 4000 cm^{-1} to record Fourier Transform Spectroscopy. Raman spectroscopy has been performed using a Renishaw 1000 spectrometer, with a 1200 lines/mm grating using the 784 nm line from a Infrared laser in the range of 400–4000 cm^{-1}, at room temperature. Curve-fitting analysis of the spectral data has been done using a commercial program, PEAK FIT to fit the Raman bands and hence the area under the peak has been calculated. AC impedance spectroscopy studies were performed on a HIOKI make LCZ meter (model 3532) in the frequency ranging from 42 Hz – 5MHz at different temperatures between 303K and 343K with stainless steel blocking electrode. ^{1}H NMR studies have been carried out using on a Bruker Spectrometer with Larmor frequency 200.13 MHz and the chemical shift has been referenced to TMS. *Preparation of cathode:* The following two cathodes were prepared by physical grinding so as to obtain a fine powder:

Cathode-1: MnO_2: C: polymer electrolyte (9:1:0.5)

Cathode-2: PbO_2:V_2O_5: C: polymer electrolyte (8:2:1:0.5)

The layered oxides MnO_2 and PbO_2 +V_2O_5 acts as the intercalation systems, graphite C was added to introduce the electronic conductivity while the addition of the polymer electrolyte helps in reducing the electrode polarization [2]. The above mixture was made in to thin pellet/disc. The thickness of the prepared pellet was ~0.79 mm. *Preparation of the anode*: Desired proportions (3:1:1) of zinc (metal) powder (Analytical Rasayan), $ZnSO_4{\cdot}7H_2O$ (GR, Himedia) and graphite powder (Himedia) were taken and mixed together and finally ground well. Then the mixture was pressed to form a thin pellet. The prepared pellet has the thickness ~0.83mm. *Cell assembly:* The polymer electrolyte was sandwiched between the anode and cathode pellets. This entire assembly was finally compacted in the sample holder. The current collectors were screwed in tightly to ensure good contact between the layers of the battery components.

3. Results and Discussion

3.1 X-ray diffraction analysis

Figure-1(a-c) represents the XRD pattern of pure PVA and PVA doped with different molar ratios of NH_4NO_3. It is clear from figure that 80PVA:$20NH_4NO_3$ polymer electrolyte has high amorphous nature (revealed from the decreased in intensity and an increased in broadness) [3] when compared to other electrolytes. Also, Peaks

corresponding to pure NH_4NO_3 [JCPDS file number 47-0865] has been found to be absent in the complex indicating a complete dissociation of salt in the polymer matrix

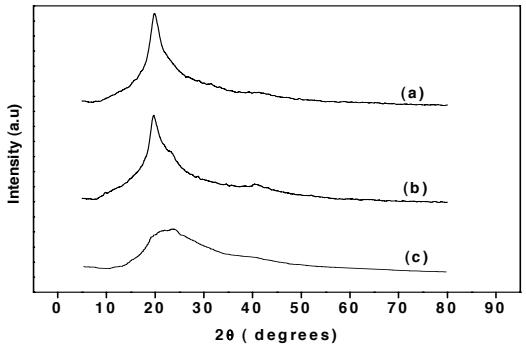

Fig. 1. XRD pattern of (a) pure PVA and PVA- NH_4NO_3 polymer electrolytes (b) 90:10, (c) 80:20

3.2 Differential scanning calorimetry analysis

The DSC plot for pure PVA (casted in DMSO) and PVA-NH_4NO_3 polymer electrolytes are shown in figure-2i and figure-2ii respectively. The observed glass transition temperature, T_g (mid-point of the endothermic step like change) of PVA was less than the reported value [7]. This is due to the plasticization of DMSO in the host polymer matrix. A very low T_g of 321K has been found for 20mol% NH_4NO_3 doped PVA.

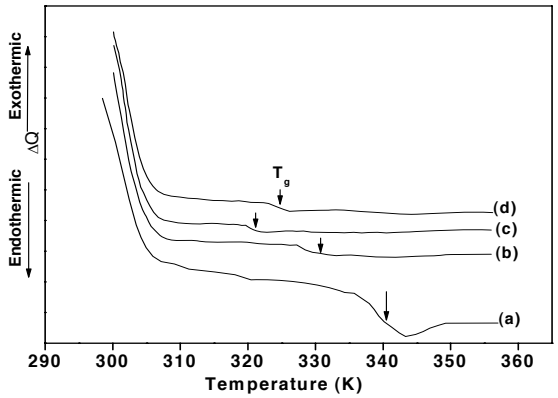

Fig. 2. DSC plot of (a) DMSO casted PVA film and different compositions of PVA-NH_4NO_3 (b) 90:10 (c) 80:20 (d) 75:25

This may be due to the softening of the complexation by the guest salt which beneficiates the easy proton transport. However for 25mol% NH_4NO_3 doped PVA, the T_g was found to be increased to 325K which may be due to the presence of some undissociated salt in the host polymer matrix.

3.3 Raman spectroscopic analysis

Figure-3 (a-g) represents the Raman spectra of pure PVA and PVA doped with different molar ratios of NH_4NO_3 in the region of 0-3500cm^{-1}. It has been observed that the intensity of the Raman band corresponding to C-C stretching vibration at 850$cm^{-1}$and 908cm^{-1}in the pure polymer electrolyte decreases with increase of NH_4NO_3 concentration. The significant changes in the C-C vibrational band can be associated with the formation of ionic bond with less polarization [8]. The 1147cm^{-1} band corresponding to ester oxygen C(O)–O–C is clearly affected by the introduction of NH_4NO_3 in to the polymer matrix which can be associated with a change in the local conformation of the polymer upon complexation.

This change in crystallinity of the polymer on the addition of the salt has been confirmed by broadening (indication of amorphous nature) [9] of the Raman modes at 1445$cm^{-1}$and 1366cm^{-1} which have been attributed to mixture of C-H bending and O-H bending vibrations. The band corresponding to the free carbonyl stretch at 1730cm^{-1} has been affected by the introduction of NH_4NO_3 which suggests the coordination between the carbonyl carbon and NO_3^- anion.

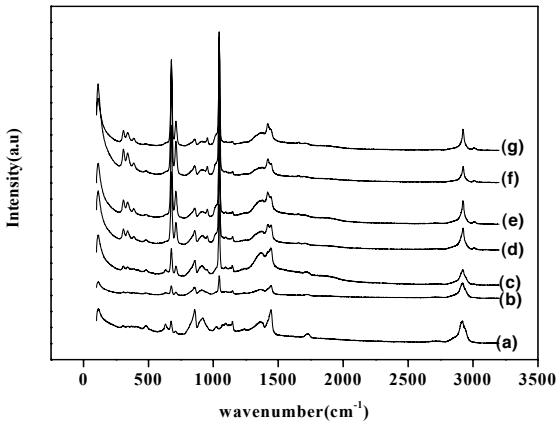

Fig. 3. Raman spectra of (a) pure PVA and different compositions of PVA-NH_4NO_3 polymer electrolytes (b) 95:05 (c)90:10 (d)85:15 (e) 80:20 (f) 75:25 (g)70:30 in the region of 0-3500cm^{-1}

The C-H stretching (at 2914cm^{-1}) band of pure PVA has been shifted in the complexed system in the NH_4NO_3 doped polymer electrolytes. This may be due to the interaction of anion with molecular complex species. The 3022cm^{-1} peak corresponding to the fundamental vibrational mode υ_1 (A_1) of NH_4^+ ion [10] has been found be present in the salt doped system with increasing intensity. To study the ion-ion interactions, it is usual to investigate the vibrational modes of the NO_3^- anion because its spectral mode is clearly dominant and different from the other vibrational modes. Figure-4 shows the deconvoluted spectra of NH_4NO_3 doped polymer electrolytes. Three bands have been observed at 1042cm^{-1}, 1046cm^{-1}, and 1049cm^{-1} while fitted by Lorentzian fit. These bands correspond to free NO_3^- ion, contact-ion pair (NH_4^-… NO_3^-) and higher ion aggregates respectively.

The fraction of ionic species in PVA- NH_4NO_3 as the function of NH_4NO_3 concentration has been shown in figure-5. The area under each peak is proportional to the relative concentration of these kinds of ionic species. The concentration of all the three ionic species increases gradually with increasing salt concentration. However the free NO_3^- ion which has been dominant upto 20mol% of NH_4NO_3 concentration has been found to be decreased beyond that. This is due to the formation of ion aggregates lowers the number of mobile charge carriers which accounts for the decrease in conductivity. Hirankumar *et al*. [11], also observed the same effect, the formation of ion aggregates in the PVA-NH_4SCN electrolyte system. Three bands at

383cm^{-1}, 335cm^{-1} and 306cm^{-1} corresponding to in-plane, and the out-of-plane bending of the S=O bond and the in-plane C-S-C bending of DMSO respectively are found in all the polymer electrolytes with increasing intensity. This reveals the presence of residual DMSO in the polymer electrolytes [12].

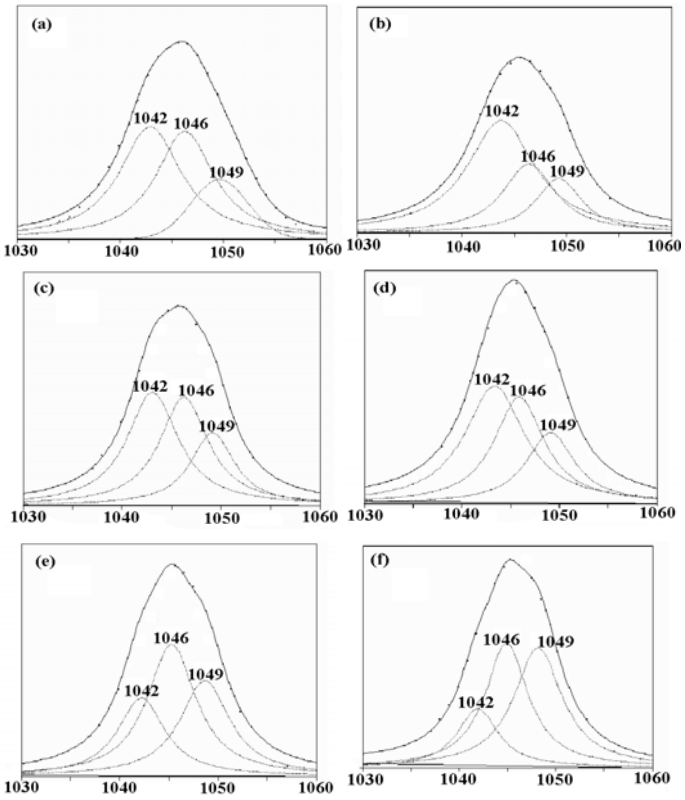

Fig. 4. Deconvoluted peak of υ_1 vibration of NO_3^- anion for different compositions of PVA-NH_4NO_3 polymer electrolytes (a) 95:05 (b) 90:10 (c) 85:15 (d) 80:20 (e) 75:25 (f) 70:30

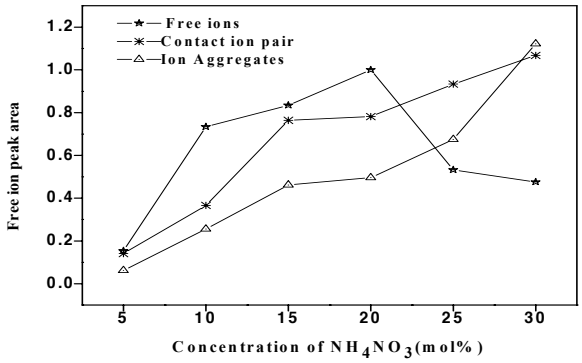

Fig. 5. Variation of peak area of ionic species as the function of NH_4NO_3 concentration

3.4 ^{1}H NMR spectroscopic analysis

Solid state NMR provides an insight into the different chemical environments in the polymer matrix and provides information about the ionic structure, mobility of the charge carriers and also gives information about the interaction between the polymer and the salt in the polymer electrolytes [13-14]. Figure-6 represents the deconvoluted spectra of pure PVA at 343K. The sharp peak centered at 2.9 ppm is attributed to methyl proton [15] of the residual solvent DMSO which acts as a plasticizer thereby enhancing the polymer chain flexibility. The peak centered at 3.8 ppm is attributed to the alcoholic proton of the host polymer [16]. The figure-7 represents the deconvoluted ^{1}H NMR spectra of the different compositions of the polymer electrolytes at 343K. The changes in the chemical shift have also been observed in the above mentioned peaks which strongly prove the interaction between the salt, solvent and the host polymer matrix.

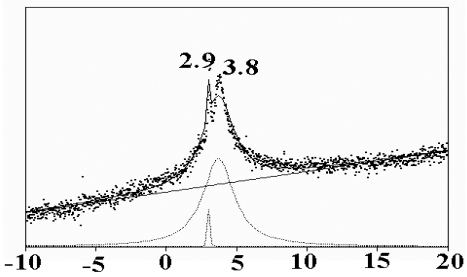

Fig.6. Deconvoluted ^{1}H NMR spectra of pure PVA at 343K

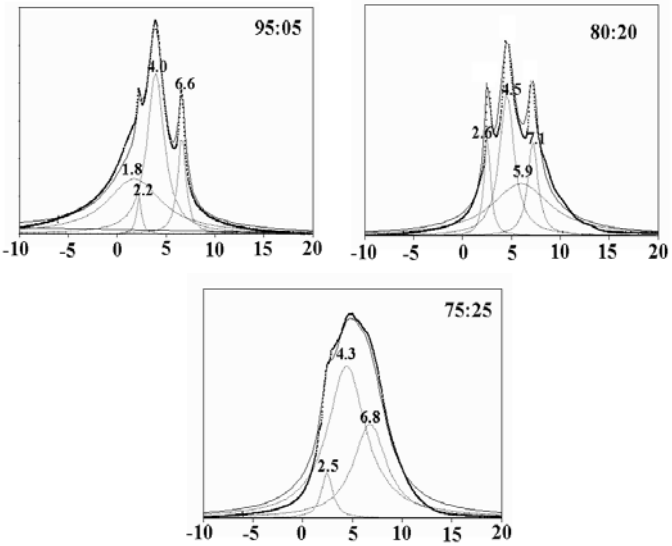

Fig.7. Deconvoluted ^{1}H NMR spectra of different compositions of PVA- NH_4NO_3 polymer electrolytes at 343K

Also, new peak at ~ 7.0 ppm attributed to ammonium proton [17] has been observed in the salt doped system. The intensity of ammonium ion peak has been found to be higher while its linewidth has been found to be the least for 80PVA-20NH_4NO_3 polymer electrolyte. Thus revealing the presence of more mobile NH_4^+ ions in the above mentioned polymer electrolyte system. The intensity of ammonium ion peak decrease in 75PVA-25NH_4NO_3 polymer electrolyte system revealing the presence of ion aggregates.

3.5 AC impedance analysis

Cole- Cole plot: Figure-8a shows the Cole- Cole plot (Nquist plot) of pure PVA and PVA-NH_4NO_3 polymer electrolyte doped with different concentration of NH_4NO_3 at 303K. The impedance plot shows a high frequency semi-circle and a low frequency spike. The high frequency semi-circle is due to the parallel combination of bulk resistance (due to migration of protons) and bulk capacitance (due to immobile polymer chains).

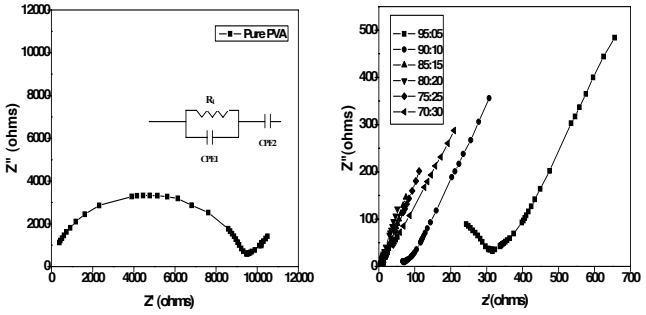

Fig.8a. Impedance plots for pure PVA and different compositions of PVA-NH_4NO_3 at 303K

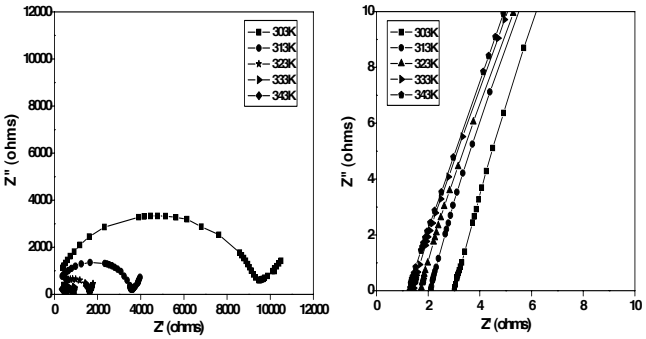

Fig.8b. Impedance plots for PVA and 80PVA- 20 NH_4NO_3 polymer electrolytes at different temperatures

Beyond 5 mol% NH_4NO_3 doped PVA, the semi-circle disappears suggesting that only the resistive component of the polymer prevails. The bulk resistance can be calculated from the intercept of high frequency semi-circle or the low frequency spike on the Z'-axis. The ionic conductivity values of the electrolytes are calculated by using the equation: $\sigma = l/R_b A$, where l, A are the thickness and known area of the electrolyte film & R_b is the bulk resistance of the electrolyte film. The ionic conductivity for pure PVA at 303K ($\sim 10^{-6}$ Scm^{-1}) has been higher than the reported value ($\sim 10^{-10}$ Scm^{-1}) because of the plasticizing effect of DMSO in the sample, the presence of which is confirmed from the Raman and ^1H NMR spectroscopic studies discussed in the earlier sections. The solvent, DMSO acts as a simple, classical plasticizer and hence it may be promoting the ion dissociation step allowing more ionic carriers to move freely inside the electrolytes so as to raise the ionic conductivity of the electrolyte [1]. The highest conductivity at 303K is found to be $7.5 \times 10^{-3} Scm^{-1}$ for 20mol%NH_4NO_3 doped PVA. From figure-8b, it has been found that as the temperature increases, the bulk resistance R_b decreases resulting in an increase in the value of ionic conductivity.

Temperature dependence of Ionic conductivity: From figure-9, it has been observed that the conductivity values of all the complexed system do not show any abrupt jump with temperature, indicating that there is no phase transition in the structure of the prepared polymer electrolytes within the measured temperature range.

Compositional dependence parameters: From figure-10, it has been found that the conductivity increases with increasing NH_4NO_3 concentration and reaches a maximum value at 20mol% (attributed to the increase in number of mobile charge carriers and also to the increase in amorphous nature of the polymer electrolyte) and there after decreases (due to the influence of ion pairs and ion aggregation leading to the formation of ion clusters) [18-19]. Figure-11 shows that FWHM is least for the PVA doped with 20mol% NH_4NO_3 polymer electrolyte possessing highest conductivity

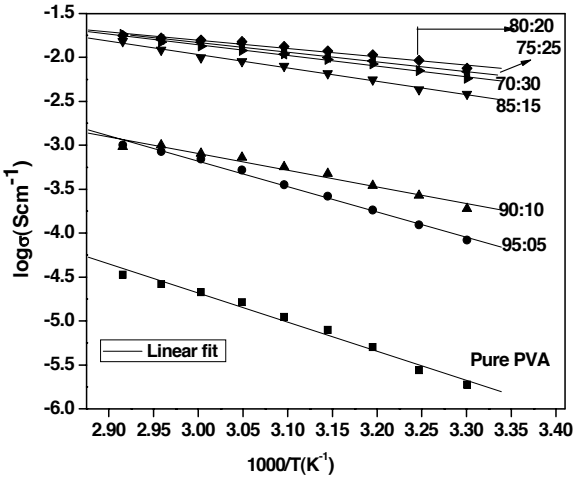

Fig.9. Temperature dependence of ionic conductivity of (a) pure PVA and different compositions of PVA-NH_4NO_3

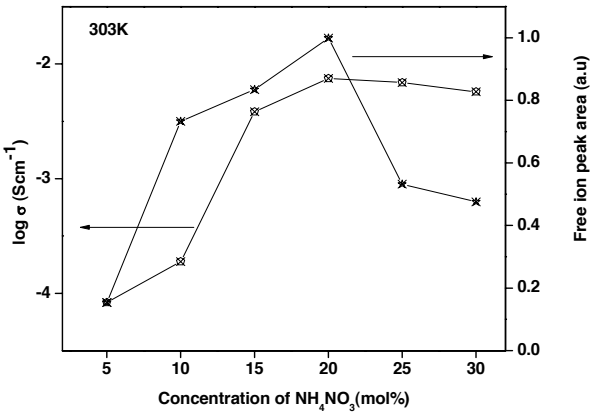

Fig.10. Variation of ionic conductivity and free ion peak area with NH_4NO_3 concentration at 303K

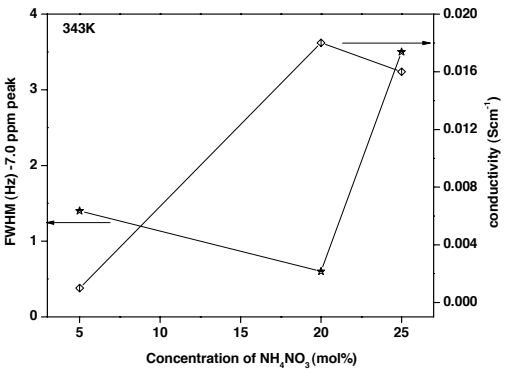

Fig.11. Variation of the FWHM of NH_4^+ peak observed in ^1H NMR study and the conductivity with salt concentration at 343K

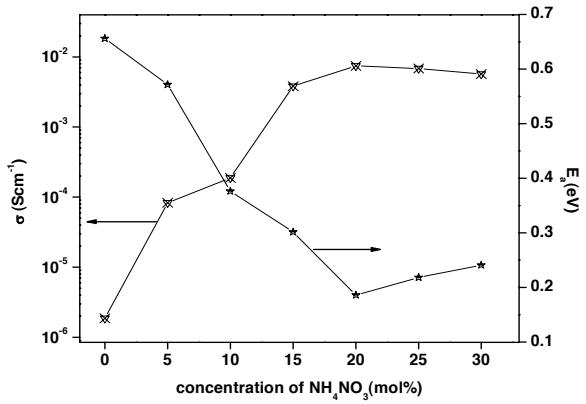

Fig.12.Variation of conductivity and Activation Energy as a function of NH_4NO_3 concentration

Figure-12 shows that the highest conductivity polymer electrolyte (80PVA-20NH_4NO_3) has the lowest activation energy (~0.19eV).It is noteworthy that the polymer electrolyte with low values of activation energies are desirable

3.6 Cell configuration

Among the prepared polymer electrolytes under study, 80PVA-20 NH_4NO_3 possess highest conductivity. Hence the cell was constructed using 80PVA:20 NH_4NO_3 polymer electrolyte. The cell, so obtained has the following below configuration.

Cell 1: Zn+$ZnSO_4.7H_2O$|80PVA: 20NH_4NO_3 |MnO_2+C + PE

Cell 2: Zn+$ZnSO_4.7H_2O$|80PVA:20NH_4NO_3|V_2O_5+PbO_2+PEC

Discharge characteristics: Open circuit voltage (OCV) values of the cell-1 and cell-2 are respectively ~1.33 V and ~1.92V. The cells were allowed to stabilize for certain duration to attain a constant voltage.

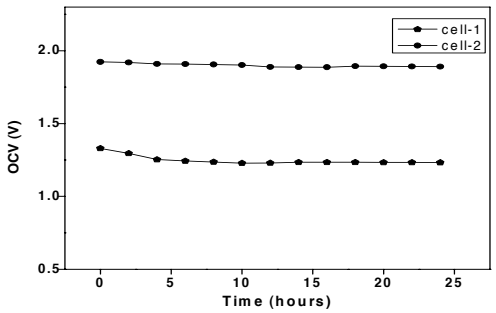

Fig.13. Open circuit voltage (OCV) as a function of time

The variation in the open circuit voltage for both cells was monitored for 24 hours and presented in figure-13. Both the cells donot show much decline in the open circuit voltage thus revealing the less shelf discharge of the cells. The stabilized voltage of 1.23V and 1.89V has been observed for cell-1 and cell-2 respectively. After the attainment of stabilized voltage, both the cells were discharged through 100kΩ and 1MΩ loads at room temperature.

Figure-14a and Figure-14b shows respectively the cell-potential variation as a function of time for the 100kΩ and 1MΩ load resistances respectively. It has been found that during discharge, the cell voltage of both cells decreases initially, remains constant for a particular duration (time of stable performance of the cell) after which there is a decline in voltage. The initial decrease in cell voltages may be due to the activation polarization [20]. When discharged with high load resistance (i.e., 1MΩ), the time of stable performance of both the cells are longer when compared to discharge with low load resistance (100kΩ). In other words, both the cells perform fairly well when discharge through a high load resistance (i.e., 1MΩ) rather than low load resistence (i.e., 100kΩ) (relatively quick discharge has been observed).

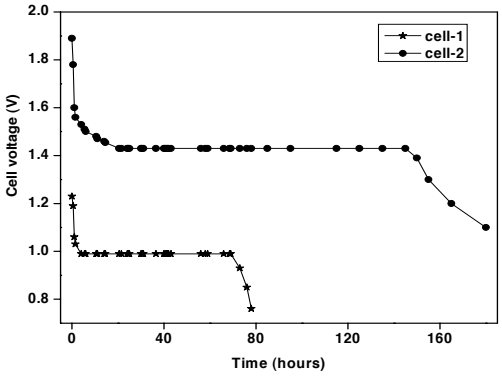

Fig.14a. Discharge curves for cells-1 and 2 using 100K

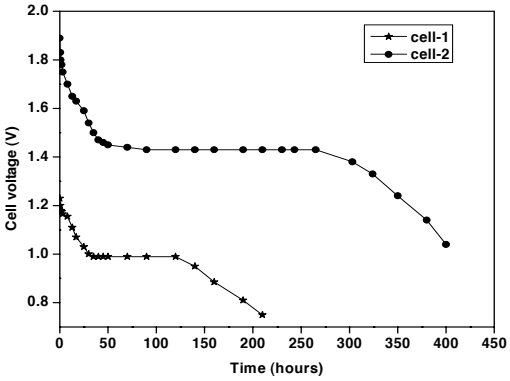

Fig.14b. Discharge curves for cells-1 and 2 using 1MΩ

While discharging through 1MΩ load, the voltage value of cell-1 remains constant at 0.99 V for ~86 hours whereas cell-2 sustains its stable voltage of 1.43 V for ~215 hours. The region in which the cell voltage remains constant is called as the "plateau region". Beyond the plateau region, voltage value of both the cells drops again. Table I lists few important cell parameters. The energy density observed for the cell-2 in the present study (7.9 $Whkg^{-1}$) is high than earlier reports [2, 21-22].

Rechargeability of cells: For rechargeability studies, the cell was allowed to discharge for a time; *t* till its voltage dropped to 20% of the initial value and then it was put to "charge" cycling. For this, the load is removed and the cell is charged using a constant current source (using Keithley 2400 source meter) compensate for the charge withdrawn from the cell during its "discharge" cycle. A typical experimental study of the rechargeability of the cell under 100KΩ load resistance is shown in Figure-15. It is clear from Figure-15 that the rechargeability can be attained without much loss of voltage ie., the cell regains its initial value after recharging.

Table I: Important cell parameters

Cell parameters	***Measured values for discharge at***			
	1 MΩ		***100kΩ***	
	Cell-1	***Cell-2***	***Cell-1***	***Cell-2***
Cell area (cm^2)	1.18	1.17	1.17	1.16
Cell weight (mg)	476.2	476	475.9	475.8
cell diameter (cm)	0.8	0.8	0.8	0.8
Cell thickness (cm)	0.070	0.068	0.067	0.065
OCV (V)	1.23	1.89	1.23	1.89
*Discharge time (h)	105	175	65	124.5
Current density (μAcm^{-2})	10.2	12.8	10.3	12.9
*Discharge capacity (mAh)	1.3	2.6	0.8	1.9
*Power density ($mWkg^{-1}$)	25	45.1	25	45.1
*Energy density ($Whkg^{-1}$)	2.6	7.9	1.6	5.6

* Parameters calculated for the stable plateau region

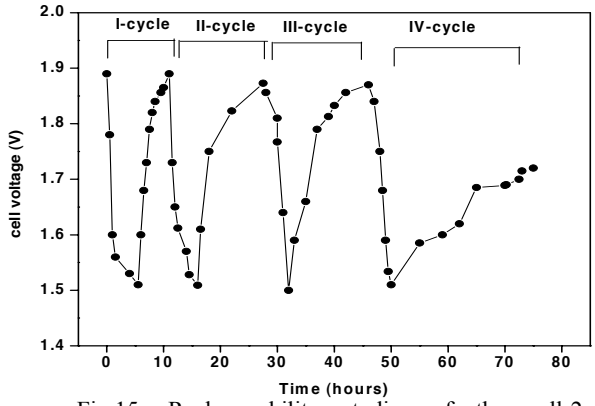

Fig.15. Rechargeability studies of the cell-2 discharged using 100KΩ load resistance and charged using 15μA constant current source

Rechargeability up to 3 cycles without significant loss in the voltage has been observed. It may be remarked that the layered materials like PbO_2 and V_2O_5 of the anode can intercalate the mobile H^+ ion (coming from the electrolyte during discharge) between its layers and de-intercalate the same during the charge cycle. However in 4th cycle, the cell voltage can't be regained as before. Also the time for retaining the cell voltage increases rapidly with recharge cycles. The above observation may be due to the following reasons: (i) the inability of the anode to supply copiously the protons to the electrolyte; (ii) the cathode might have undergone some structural changes (i.e.,topotactic nature might be affected) during insertion and extraction of the protons;(iii) though polymer electrolyte (being thin and flexible provides good electrochemical compatibility between the electrodes) was used, the solid electrodes in the present study might have developed some interfacial resistances.

4. Conclusion

The optimized polymer electrolyte (with high conductivity, high amorphous nature, low activation energy, more free ion concentration, and low glass transition temperature) - 80PVA: $20NH_4NO_3$ has been applied for proton battery. The discharge characteristics of both the cells reveal that the cell performance is fairly well when discharge through 1MΩ than through 100KΩ load. The cell-2 shows rechargeability up to 3 cycles without significant loss in the voltage. The obtained highest energy density and current density in the present study were 7.9 $Whkg^{-1}$ and of 12.8μAcm^{-2} respectively.

[1] D. R. MacFarlane, F. Zhou, M. Forsyth: Solid State Ionics **113-15** (1998) 193.
[2] R. C. Agrawal, S. A. Hashmi: Ionics **13** (2007) 295.
[3] R. M. Hodge, G. H. Edward: Polymer **37** (1996) 1371.
[4] Z. Wang, B. Huang, R. Xue: Solid State Ionics **121** (1999) 141.
[5] S. Rajandran, M. Sivakumar: Mater. Lett. **58** (2004) 641.
[6] A. Awadhia, S. L. Agrawal: Solid State Ionics **178** (2007) 951.
[7] J. Brandrup, E. H. Immergnt: Polymer Handbook, Interscience; Newyork, 1996, p-III-72.
[8] G. A. Nazri, M. D. Mac Arthur, J. F. O' Gara, R. Aroca: Solid State Ionics II. In: Materials Research Society Symposium Proc., G.A.Nazri, G.F. Shriver, R.A. Huggins, M. Balkansi, 1991, p. 163.
[9] D. Martin-Vosshage, B. V. R. Chowdari: Solid State Ionics **62** (1993) 205.
[10] A. M. Heyns, K. R. Hirsch: J. Chem. Phys **73** (1980) 105.
[11] G. Hirankumar, S. Selvasekarapandian, J. Kawamura, N. Kuwata, O. Kamishima, T. Hattori: Proc. of 10th Asian Conference on Solid State Ionics, B.V.R. Chowdari, M.A. Careem, M.A.K.L. Dissanayake, R.M.G. Rajapakse, V.A. Seneviratne, 2006. p. 608.
[12] Z. Wang, B. Huang, S. Wang, R. Xue, Xuejie: Electrochim. Acta **42** (1997) 2611.
[13] S. Selvasekarapandian, G. Hirankumar, J. Kawamura, N. Kuwata, T. Hattori: Mater. Lett. **59** (2005) 2741.
[14] C. H. Kim, J. K. Park: Solid State Ionics **116** (1999) 53.
[15] V. Mahalingam: Polyhedron **27** (2008) 2743.
[16] Pavia, Lampman, Kriz (Eds.), "Introduction to spectroscopy" (3rd edition).
[17] F. Michael, E. Astrid, J. C. Schwalowsky, B. Ulrich: Solid State Nuclear Magnetic Resonance **17** (2000) 76.
[18] G. Hirankumar, S. Selvasekarapandian, M. S. Bhuvaneswari: J. Solid State Electrochem. **10** (2006) 193.
[19] G. Hirankumar, S. Selvasekarapandian, N. Kuwata, J. Kawamura, T. Hattori: J. Power Sources **144** (2005) 262.
[20] H. J. De Bruin: J. Am. Ceramic. Soc. **14** (1978) 20.
[21] K. Pandey, N. Lakshmi, S. Chandra: J. Power Sources **76** (1998) 116.
[22] R. Pratap, B. Singh, S. Chandra: J. Power Sources **161** (2006) 702.